



OPEN ACCESS

EDITED BY

Kaijun Zhao,
Tongji University, China

REVIEWED BY

Jinchao Xia,
Henan Provincial People's Hospital, China
Yigit Can Senol,
University of California, San Francisco,
United States

*CORRESPONDENCE

Pinjing Hui
✉ pinjing-hui@163.com

RECEIVED 18 September 2024

ACCEPTED 24 March 2025

PUBLISHED 07 April 2025

CITATION

Xu X, Yan Y, Qu Y, Zhang L and Hui P (2025)
Predicting vessel recanalization in extracranial
internal carotid artery dissection: a
nomogram based on ultrasonography and
clinical features.
Front. Neurol. 16:1498182.
doi: 10.3389/fneur.2025.1498182

COPYRIGHT

© 2025 Xu, Yan, Qu, Zhang and Hui. This is an
open-access article distributed under the
terms of the [Creative Commons Attribution
License \(CC BY\)](https://creativecommons.org/licenses/by/4.0/). The use, distribution or
reproduction in other forums is permitted,
provided the original author(s) and the
copyright owner(s) are credited and that the
original publication in this journal is cited, in
accordance with accepted academic
practice. No use, distribution or reproduction
is permitted which does not comply with
these terms.

Predicting vessel recanalization in extracranial internal carotid artery dissection: a nomogram based on ultrasonography and clinical features

Xinchun Xu^{1,2,3}, Yanhong Yan^{1,2}, Yafeng Qu³, Lianlian Zhang^{1,2}
and Pinjing Hui^{1,2*}

¹Department of Neurosurgery, The First Affiliated Hospital of Soochow University, Suzhou, China,

²Department of Stroke Center, The First Affiliated Hospital of Soochow University, Suzhou, China,

³Department of Ultrasound, The Affiliated Zhangjiagang Hospital of Soochow University, Suzhou, China

Background: Extracranial internal carotid artery dissection (EICAD) is a prominent factor in ischemic stroke in young patients, and vessel recanalization is correlated with stroke recurrence. We propose to determine the possible association between carotid duplex ultrasound (CDU) features, clinical factors, and vessel recanalization in EICAD patients.

Methods: In the current retrospective study, data from 202 patients diagnosed with EICAD by CDU and confirmed by computed tomography angiography (CTA) or high-resolution magnetic resonance imaging (HRMRI) were encompassed. Patients were randomized 7:3 into training cohort ($n = 142$) and validation cohort ($n = 60$). The least absolute shrinkage and selection operator (LASSO) regression analysis and multivariate logistic regression analysis were used to build a nomogram to predict recanalization. At last, we assessed the performance of the nomogram with an area under the receiver operating characteristic curve (AUC), calibration curve, decision curve analysis (DCA), and clinical impact curve (CIC).

Results: The nomogram included CDU features (intramural hematoma, Intraluminal thrombus, and stenosis degree) and age, with AUC values of 0.906 (95% CI: 0.857–0.946) and 0.903 (95% CI: 0.820–0.963) in the training cohort and the validation cohort, respectively. Using a probability cutoff of 0.5 derived from the Youden index, patients were stratified into high-risk (recanalization probability <50%) and low-risk groups ($\geq 50\%$). DCA showed that the nomogram performed significantly better across various threshold probabilities, and CIC demonstrated that the nomogram offers superior net benefit across a broad range of threshold probabilities, indicating its significant predictive value.

Conclusion: A nomogram depended on CDU and clinical features could accurately predict recanalization in EICAD patients. The nomogram may facilitate early identification of high-risk patients and personalized therapeutic strategies.

KEYWORDS

extracranial internal carotid artery dissection, vessel recanalization, carotid duplex ultrasound, predictive model, nomogram

Introduction

Extracranial internal carotid artery dissection (EICAD) is a disorder characterized by the passage of blood via a rip in the arterial wall layers, resulting in the blood entering the space between these layers, causing the carotid wall to separate into two layers and interfering with blood flow, which can lead to secondary stenosis or aneurysmal dilatation (1). Carotid artery dissection (CAD) accounts for around 25% of strokes in young individuals, making it a significant factor in stroke occurrence among individuals in their youth and middle age (2). Therefore, the accurate diagnosis and effective treatment of carotid artery dissection, as well as the enhancement of patients' prognosis, are of crucial in clinical practice. Digital subtraction angiography (DSA) has traditionally been considered the most reliable method for diagnosing EICAD. However, this technique is an invasive examination and cannot clearly show the morphology of arterial wall, so it has certain limitations in the clinical diagnosis and treatment process (3). In recent times, high-resolution magnetic resonance imaging (HRMRI) has been increasingly employed in clinical practice. It has a high detection rate for intramural hematoma and can clearly show the structure of the vessel wall. However, it is time-consuming (4). Carotid Doppler ultrasound (CDU) has emerged as a valuable diagnostic modality for the evaluation of EICAD. It offers several advantages over other imaging techniques, such as being non-invasive and cost-effective, and it can observe the lumen and artery wall of the extracranial internal carotid artery in real-time. Therefore, CDU is of great value in evaluating the variations in vascular wall structure of EICAD patients.

Previous studies have been conducted on the recanalization rate of CAD (5–7), while limited attention has been given to the influence factors of recanalization. Furthermore, the nomogram is progressively employed as a visual aid for the purpose of illness prevention. However, few studies have combined CDU characteristics and clinical factors to establish a nomogram to evaluate the recanalization of EICAD. We aim to combine CDU features and clinical factors to identify those factors that are significantly correlated to vessel recanalization and to establish a nomogram to forecast the recanalization probability.

Materials and methods

Patient data

This study was approved by the Ethics Committee of the first affiliated hospital of Soochow University (No. 2021196). The individuals provided informed consent before enrolling in the study. The clinical and imaging data of EICAD patients were admitted from August 1, 2015, to June 30, 2023. The inclusion criteria were: (1) patients with suspected EICAD who received CDU examinations and were confirmed by following HRMRI and/or CTA; (2) patients with available follow-up ultrasound examinations for assessment. Clinical suspicion of EICAD depended on one or more of the following signs: neck pain, headache, and Horner's syndrome. Patients were excluded if: (1) patients had bilateral or multiple-segment CAD; (2) patients had incomplete medical records or missing data necessary for analysis; and (3) patients had contraindications to anticoagulant or antiplatelet therapy. In our research, a total of 202 individuals with EICAD were

included. All patients received anticoagulant therapy (warfarin, dabigatran, or rivaroxaban, maintained at an international normalized ratio [INR] of 2.0–3.0) or antiplatelet therapy (aspirin 100 mg/day and/or clopidogrel 75 mg/day) upon initial diagnosis. The choice of therapy was guided by protocols, considering factors such as dissection severity and bleeding risk (8). Subsequently, the patients who had joined were allocated into two groups, namely a training group ($n = 142$) and a validation group ($n = 60$), using a randomization process with a ratio of 7:3. Figure 1 displays the specifics of the research design.

Data collection

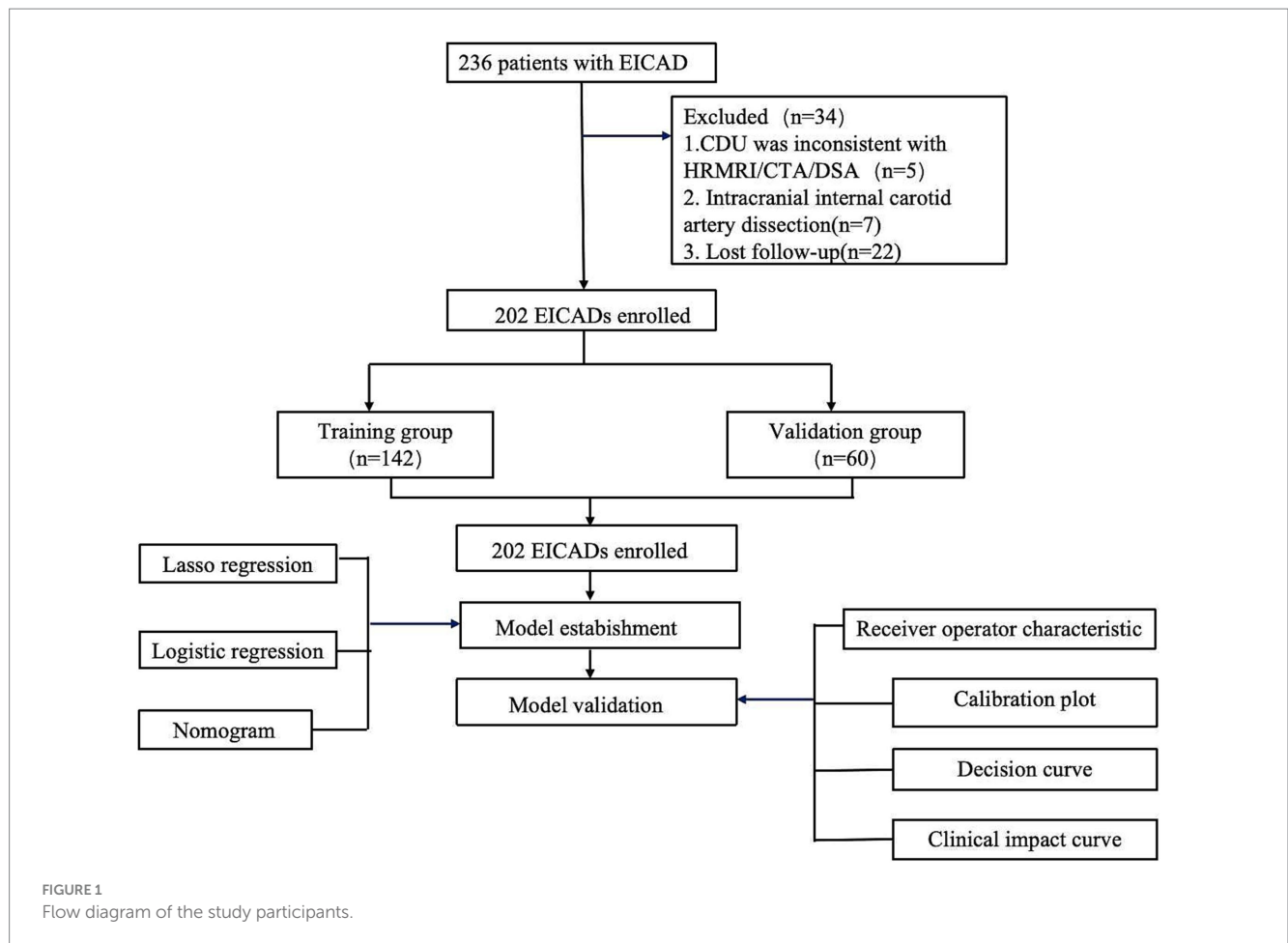
The following demographic and clinical data were obtained: age, gender, neck pain, headache, Horner's syndrome, hypertension, diabetes, smoking, neck trauma, prior stroke, low-density lipoprotein cholesterol (LDL-C, mmol/L), High-density lipoprotein cholesterol (HDL-C, mmol/L), Total cholesterol (TC, mmol/L), triglycerides (mmol/L), glycated hemoglobin (HbA1c), homocysteine (HCY, umol/L), high-sensitivity C reactive protein (hs-CRP, mg/L), the National Institutes of Health Stroke Scale (NIHSS), medical treatment (antiplatelets, anticoagulant, or treatment with both agents), and initial and follow-up imaging.

Imaging examinations

CDU imaging was conducted employing an iU-Elite scanner (Phillips Medical System, Bothell, Washington) that has a high-frequency L9-3 probe. All examinations were performed by a 10-year experienced sonographer who specialized in vascular ultrasound. During the examination, the patient was positioned in a supine posture with his head rotated toward the opposite carotid artery. Two-dimensional real-time imaging was performed to scan the transverse section first and then the longitudinal section.

The CTA examination used a 320-row-detector CT scanner (Aquilion ONE, Toshiba Medical Systems, Tokyo, Japan) with a high-spaced spiral scan mode. The imaging parameters were as follows: 100 kV tube voltage, 1.0 spacing, 3 mm slice thickness, 3 mm gap, rotation time of 0.5 s, and scanning time of 3–4 s, delay time of 2 s. After routine scanning, patients received 40 mL of intravenous iodine contrast agent (Isovue-M[®], United States) at 4–5 mL/s, followed by 50 mL of saline at the same injection rate. All images were transmitted to the workstation for post-processing of multiplanar reconstruction (MPR), maximum density projection (MIP), surface reconstruction (CPR), and volume reorganization (VR).

The patients received HRMRI utilizing a 3-Tesla MRI system (Ingenia, Philips Healthcare, Best, the Netherlands) equipped with an eight-channel integrated head and neck coil. The imaging procedure encompassed T1W black-blood (BB) sequence, 3D time-of-flight (TOF) MRA, fat-suppressed (FS) T2-weighted BB imaging, and proton-density-weighted volume isotropic turbo-spin-echo acquisition (PD-VISTA) sequences. The T1W-BB and T2W-BB sequences were obtained in the axial orientation. The PD-VISTA pictures were obtained in the coronal orientation. The following variables were used: 3D TOF MRA with a repetition time (TR) of 15 ms and an echo time (TE) of 3.5 ms, the field of view (FOV) was



220 × 128 × 148 mm³, with a matrix size of 512 × 512, and the total scanning time was 3.5 min; PD-VISTA: TR of 34 ms and TE of 2,000 ms, the FOV was 189 × 162 × 40 mm³, with a matrix size of 480 × 480, and the total scanning time was 2 min 40 s. T1W-BB has a scanning time of 4 min 58 s with a TR/TE of 20 ms/968 ms, FOV of 100 × 100 × 17 mm³, and a matrix size of 352 × 352; FS-T2W-BB has a scanning time of 4 min 13 s with a TR/TE of 2,432 ms/40 ms, FOV of 100 × 100 × 15 mm³, and a matrix size of 384 × 384.

Image analysis

Two experienced radiologists, each with over five years of diagnostic experience, reviewed baseline and follow-up imaging independently using PACS workstation. On CDU and HRMRI, the presence of EICAD was defined if images had either (9–12): (1) double lumen; (2) intimal flap; (3) intramural hematoma; (4) intraluminal thrombus; or (5) a tapering stenosis with distal occlusion with no atherosclerotic disease exists. On CTA, the presence of EICAD was defined as one of these features: (1) intimal flap; (2) an enlargement of the dissection artery; (3) dissecting aneurysm; or the lumen is small and irregularly formed, with a thrombus forming a crescent shape around it. There is also a thin ring of enhanced tissue around the thrombus (13, 14). Stenoses of the EICA were defined based on guidelines by North American Symptomatic Carotid Endarterectomy Trial (NASCET) (15). The degree of stenosis was categorized based on

the following ranges: mild (<50%), moderate (50–69%), severe (70–99%), and complete occlusion.

Outcome definition

Recanalization was defined as the reopening of the injured vessels with no vascular abnormalities, and blood flow velocity and spectral morphology were normal, which was assessed using follow-up CDU (Figure 2). Patients underwent initial CDU assessment at 1 month post-diagnosis, followed by serial evaluations every 3 months until recanalization was confirmed or the 1-year endpoint was reached.

Statistical analysis

The statistical analyses were conducted employing the R program (version 4.2.2; R Foundation for Statistical Computing, Vienna, Austria) and its related data packages. The dataset was partitioned into training and validation cohorts employing a random allocation ratio of 7:3, and the variables were then examined. The continuous data were reported as the mean and standard deviation (SD) or the median (interquartile range [IQR]), whereas the categorical data were reported as numbers expressed as a percentage (%). The categorical variables were analyzed employing either the Pearson chi-square test or Fisher's exact test, while the continuous variables were examined employing either the Student's

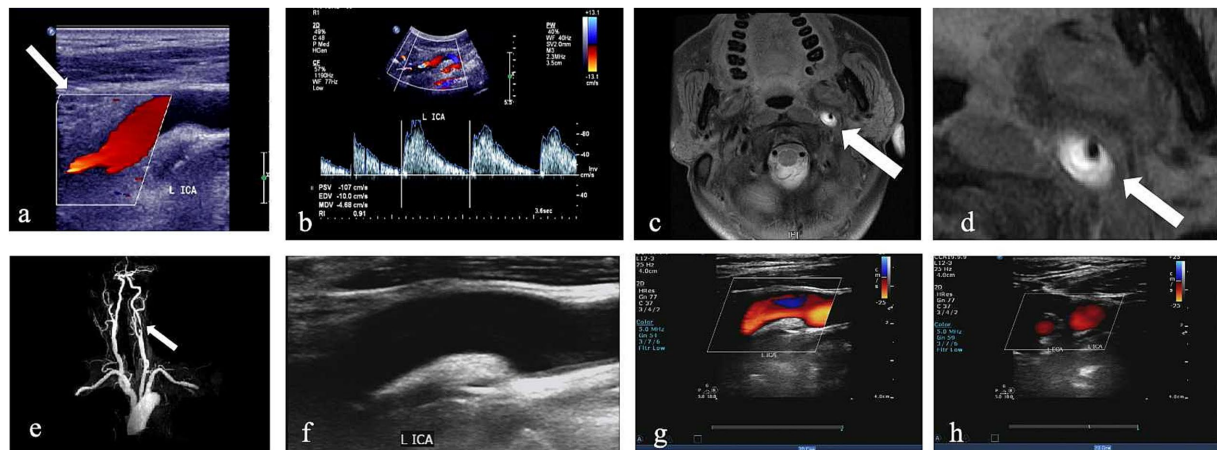


FIGURE 2
 CDU imaging for one patient with left internal CAD. **(a,b)** Greyscale and pulsed-wave Doppler with hypoechoic intramural hematoma (white arrow) and lumen narrowing. **(c,d)** Corresponding HRMRI with evidence of a crescent-shape hyperintense on axial FS-T2W images and enlarged view of FS-T2W (white arrow). **(e)** 3D time-of-flight (TOF) magnetic resonance angiography imaging. **(f–h)** CDU done 6 months later shows recanalization after treatment; the wall structure of the ICA returned to normal, and the blood flow signal was completely filled.

t-test or Mann–Whitney U test. The training cohort deployed the least absolute shrinkage and selection operator (LASSO) logistic regression analysis to identify the most suitable variables for recanalization. Subsequently, a multivariate logistic regression analysis (MVLr) was conducted by including the chosen characteristics in the LASSO regression model. The outcomes of the MVLr were used to create the ultimate forecasting model. Subsequently, we constructed a prognostic nomogram to estimate the likelihood of recanalization. The nomogram is internally verified using the training set and externally validated using the validation set. The discriminating performance of the model was determined by employing the receiver operating characteristic (ROC) curve. A calibration plot was employed to determine the correlation between the reported risk and the estimated risk. Furthermore, a decision curve analysis (DCA) was conducted to ascertain the net benefit threshold of the prediction, and clinical impact curve (CIC) were generated to assess the clinical utility and net benefits of the model exhibiting the best diagnostic accuracy. AUC values were compared using the DeLong test. The total points derived from the nomogram were translated into predicted probabilities of recanalization. Based on the Youden index calculated from the ROC curve analysis, a cutoff value of 0.5 (50% probability) was selected to stratify patients into high-risk (probability < 50%) and low-risk (probability ≥ 50%) groups for recanalization. Significance was attributed to variations when the *p*-value was < 0.05.

Results

Patient characteristics

The study included 202 patients with EICAD, of whom 90 (44.6%) achieved recanalization. The mean age of the cohort was 48.6 ± 10.9 years, with a male predominance (76.2%). Key clinical characteristics included hypertension (46.5%), diabetes (14.3%), and smoking history (31.2%). Among imaging features, intramural hematoma (IMH) was present in 62.9% of patients, intraluminal thrombus in 27.2%, and complete occlusion in 46.5%. Table 1 provides a summary of the baseline characteristics of the research population.

The patients were allocated into training and validation cohorts employing a random selection process. The training cohort included 142 individuals, while the validation cohort consisted of 60 patients at a ratio of 7:3 and summarized their CDU and clinical characteristics (Table 2). Overall, the baseline characteristics of the study population were similar between the training cohort and the validation cohort, indicating that they can be considered comparable for further analysis.

Clinical outcomes during follow-up

During follow-up, 16 out of 202 patients (7.9%) experienced cerebrovascular events. These included 12 ischemic strokes, and 4 transient ischemic attacks (TIA). Patients without recanalization had a significantly higher incidence of cerebrovascular events (13/112, 11.6%) compared to those with recanalization (3/90, 3.3%; *p* = 0.03). Most events occurred within the first 6 months post-diagnosis (14/16, 87.5%), aligning with the period of highest thrombotic risk in EICAD.

Predictive model

The candidate variables shown in Table 2 were initially included in the original model. Subsequently, LASSO regression analysis was conducted on the training cohort, resulting in the selection of seven possible predictors: age, smoking, LDL-C, treated with antiplatelets and anticoagulant, IMH, Intraluminal thrombus, and stenosis degree. The coefficients are provided in Table 3, while a graphical representation of the coefficient profile may be seen in Figure 3a. Figure 3b displays a cross-validated (CV) error curve of the LASSO regression model. The model that had the most regularized and parsimonious approach and had a CV error that was within one standard error of the minimum consisted of 7 variables.

MVLr analysis of these seven variables is shown in Table 4. The findings of the multivariate regression analysis indicated age (*p* < 0.001), IMH (*p* < 0.001), and occlusion (*p* = 0.001) as vessel recanalization risk factors.

TABLE 1 Clinical characteristics of EICAD patients.

Characteristic	Recanalization			p-value
	Overall, N = 202	yes, N = 90	no, N = 112	
Age	48.6 ± 10.9	43.1 ± 10.3	53.1 ± 9.2	<0.001
Gender				0.062
Female	48 (23.8)	27 (30.0)	21 (18.8)	
Male	154 (76.2)	63 (70.0)	91 (81.2)	
Neck pain	23 (11.4)	11 (10.0)	12 (13.3)	0.435
Headache	29 (14.4)	17 (15.2)	12 (13.3)	0.710
Hornor sign	16 (7.9)	9 (8.0)	7 (7.7)	0.946
Hypertension	94 (46.5)	41 (45.6)	53 (47.3)	0.803
Diabetes	29 (14.3)	13 (11.6)	16 (17.8)	0.214
Smoking	63 (31.2)	15 (16.7)	48 (42.9)	<0.001
Neck trauma	32 (15.8)	17 (15.2)	15 (16.7)	0.773
Prior stroke	18 (8.9)	4 (4.4)	14 (12.5)	0.046
NIHSS score	3.0 (0.0, 7.8)	4.0 (0.0, 7.5)	3.0 (0.0, 7.3)	0.934
Laboratory examination				
TC (mmol/L)	3.83 (3.22, 4.65)	3.85 (3.31, 4.65)	3.83 (2.97, 4.63)	0.245
HDL-C (mmol/L)	1.05 (0.86, 1.24)	1.04 (0.91, 1.16)	1.05 (0.81, 1.27)	0.352
LDL-C (mmol/L)	2.22 (1.65, 3.00)	2.22 (1.89, 2.95)	2.20 (1.54, 3.00)	0.309
Triglycerides (mmol/L)	9.8 (6.5,13.6)	9.6 (7.1,13.1)	10.1 (7.4,13.8)	0.412
HbA1c (%)	5.9 (5.5, 6.5)	5.6 (3.89, 6.4)	6.2 (4.1, 6.7)	0.966
HCY (umol/L)	9.4 (8.0, 11.6)	9.2 (7.7, 11.6)	9.7 (8.2, 11.2)	0.309
hs-CRP (mg/L)	2.6 (1.0, 6.3)	2.4 (0.8, 4.6)	4.0 (1.2, 9.2)	0.101
NIHSS score	3.0 (0.0, 7.8)	4.0 (0.0, 7.5)	3.0 (0.0, 7.3)	0.934
Medical treatment				
Antiplatelets	73 (36.1)	39 (43.3)	34 (30.4)	0.056
Anticoagulant	35 (17.3)	24 (21.4)	11 (12.2)	0.886
Treated with both agents	96 (47.5)	32 (35.6)	64 (57.1)	0.002
Carotid dissection imaging				
Double lumen	25 (12.4)	17 (15.2)	8 (8.9)	0.177
Intimal flap	29 (14.4)	17 (15.2)	12 (13.3)	0.710
IMH	127 (62.9)	37 (41.1)	90 (80.4)	<0.001
Intraluminal thrombus	55 (27.2)	32 (35.6)	23 (20.5)	0.017
Stenosis degree				<0.001
Mild	30 (14.9)	21 (18.8)	9 (10.0)	
Severe	40 (19.8)	25 (22.3)	15 (16.7)	
Moderate	38 (18.9)	29 (25.9)	9 (10.0)	
Occlusion	94 (46.5)	36 (33.0)	58 (64.4)	

Values are presented as mean (SD), median (25th-75th percentile), or number of patients (%). Welch Two Sample t-test; Pearson's Chi-squared test; Fisher's exact test; Wilcoxon rank sum test. EICAD, extracranial carotid artery dissection; TC, Total cholesterol; HDL-C, High-density lipoprotein cholesterol; LDL-C, Low-density Lipoprotein cholesterol; HbA1c, Glycated hemoglobin; HCY, homocysteine; hs-CRP, high sensitivity C reactive protein; NIHSS, National Institutes of Health Stroke Scale; IMH, intramural hematoma; IQR, interquartile range.

Nomogram establishment and validation

The final logistic model encompassed four autonomous variables (age, IMH, Intraluminal.thrombus, and stenosis degree) were formulated as a user-friendly nomogram (Figure 4).

The discriminating power of the prediction model was assessed using the area under the curve (AUC). The AUC was found to

be 0.906 in the training cohorts and 0.903 in the validation cohorts, indicating outstanding performance (Figure 5).

One thousand bootstrap studies were used to authenticate and calibrate the nomogram. The calibration plots of the nomogram in the various cohorts are shown in Figure 6, showing a strong connection between the observed and anticipated recanalization. The findings indicated that the original nomogram remained applicable for the

TABLE 2 Patient demographics and baseline characteristics.

Characteristic	Training Cohort N = 142	Validation Cohort N = 60	p-value
Age	48.2 ± 11.3	51.4 ± 10.1	0.212
Gender			0.926
Female	34 (23.9)	14 (23.3)	
Male	108 (76.1)	46 (76.7)	
Neck pain	16 (11.3)	7 (11.7)	0.823
Headache	21 (14.8)	8 (13.3)	0.756
Horner sign	10 (7.0)	6 (10.0)	0.573
Hypertention	64 (45.1)	30 (50.0)	0.620
Diabetes	20 (14.1)	9 (15.0)	0.685
Smoking	45 (31.7)	18 (30.0)	0.813
Neck trauma	23 (16.2)	9 (15.0)	0.689
Prior stroke	14 (9.8)	4 (6.7)	0.467
NIHSS score	3.0 (0.0, 7.0)	4.0 (1.0, 8.0)	0.558
Laboratory examination			
TC (mmol/L)	3.78 (3.16, 4.65)	3.98 (3.40, 4.80)	0.315
HDL-C (mmol/L)	1.05 (0.86, 1.21)	1.03 (0.89, 1.24)	0.803
LDL-C (mmol/L)	2.15 (1.65, 2.98)	2.29 (1.84, 3.01)	0.554
Triglycerides (mmol/L)	9.6 (7.3,12.7)	9.8 (7.6,13.1)	0.375
HbA1c (%)	5.90 (5.50, 6.90)	5.70 (5.40, 6.30)	0.181
HCY (umol/L)	9.4 (8.0, 11.6)	9.4 (7.4, 11.6)	0.730
hs-CRP (mg/L)	2.7 (1.2, 6.3)	2.5 (0.7, 6.4)	0.359
Medical treatment			
Antiplatelets	57 (40.1)	16 (26.7)	0.069
Anticoagulant	27 (19.0)	6 (10.0)	0.100
Treated with both agents	58 (40.8)	33 (55.0)	0.061
Carotid dissection imaging			
Double lumen	18 (12.7)	7 (11.7)	0.555
Intimal flap	19 (13.4)	10 (16.7)	0.587
IMH	92 (64.8)	35 (58.3)	0.386
Intraluminal thrombus	39 (27.5)	16 (26.7)	0.907
Stenosis degree			0.271
Mild	18 (12.7)	12 (20.0)	
Moderate	27 (19.0)	13 (21.7)	
Severe	25 (17.6)	13 (21.7)	
Occlusion	67 (47.2)	27 (45.0)	

Values are presented as mean (SD), median (25th-75th percentile), or number of patients (%). Welch Two Sample t-test; Pearson's Chi-squared test; Fisher's exact test; Wilcoxon rank sum test. TC, Total cholesterol; HDL-C, High-density lipoprotein cholesterol; LDL-C, Low-density Lipoprotein cholesterol; HbA1c, Glycated hemoglobin; HCY, homocysteine; hs-CRP, high sensitivity C reactive protein; NIHSS, National Institutes of Health Stroke Scale; IMH, intramural hematoma; IQR, interquartile range.

validation sets, and the calibration curve of this model closely approximated the ideal curve. This implies that the anticipated outcomes were in line with the actual observations.

Figure 7 illustrates the DCA curves associated with the nomogram. The findings indicated that the nomogram exhibited a

TABLE 3 The coefficients of LASSO regression analysis.

Coefficient	Variable
5.41624887	(Intercept)
-0.08715714	Age_level_
0.00000000	gender_level_male
0.00000000	neck pain_level_yes
0.00000000	headache_level_yes
0.00000000	Hornor sign_level_yes
0.00000000	hypertension_level_yes
0.00000000	diabetes_level_yes
-0.03472626	smoking_level_yes
0.00000000	Neck trauma_level_yes
0.00000000	prior.stroke_level_yes
0.00000000	TC_level_
0.00000000	HDL-C_level_
0.22847481	LDL-C_level_
0.00000000	HbA1c..._level_
0.00000000	HCY_level_
0.00000000	hs-CRP_level_
0.00000000	NIHSS_level_
0.00000000	Antiplatelets_level_yes
0.00000000	Anticoagulant_level_yes
-0.45366172	Treated.with.both.agents_level_yes
0.00000000	Double.lumen_level_yes
0.00000000	Intimal.flap_level_yes
-0.11460475	IMH_level_yes
-1.71225982	Intraluminal.thrombus_level_yes
0.00000000	Stenosis degree_level_Moderate
0.00000000	Stenosis degree_level_Severe
-1.59566650	Stenosis degree_level_Occlusion

greater net advantage in the validation set when the threshold probability ranged from 10 to 75%. CIC analysis showed the clinical efficacy of the predictive model. When the threshold probability is greater than 80% of the prediction score probability value, the prediction model determines that the population of recanalization is highly matched with the actual population, which confirms the high clinical effectiveness of the prediction model (Figure 8).

Risk stratification based on nomogram scores

Using the cutoff value of 0.5, 64.8% (92/142) of patients in the training cohort and 61.7% (37/60) in the validation cohort were classified as high-risk for non-recanalization. High-risk patients exhibited significantly lower recanalization rates (training: 12.0% vs. 88.0%; validation: 16.2% vs. 83.8%; $p < 0.001$) compared to low-risk patients, confirming the clinical utility of the nomogram in risk stratification.

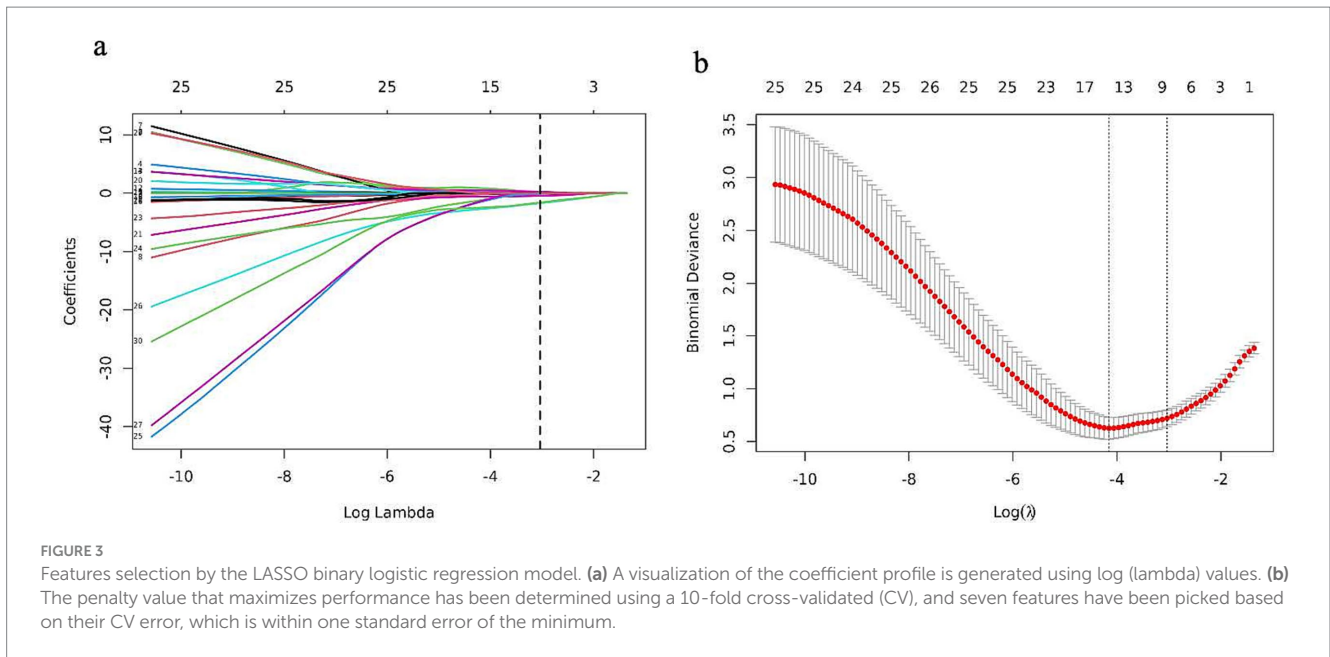


TABLE 4 Results of the multivariate logistic analysis based on the training cohort.

Variables	β	S.E	Z	p	OR (95%CI)
Age	-0.170	0.038	4.505	<0.001	0.844 (0.784,0.909)
Smoking	-0.744	0.610	1.219	0.223	0.475 (0.144,1.572)
IMH	-5.532	1.419	3.898	<0.001	0.645 (0.161,2.589)
Intraluminal thrombus	-2.556	1.324	1.930	0.054	0.078 (0.006,1.040)
Stenosis degree					
Mild					Ref
Moderate	-1.380	0.908	1.519	0.787	0.252 (0.042,1.493)
Severe	-0.439	0.709	0.619	0.536	0.645 (0.161,2.589)
Occlusion	-2.747	0.819	3.352	0.001	0.064 (0.013,0.320)

IMH, intramural hematoma; OR, odds ratio; CI, confidence interval.

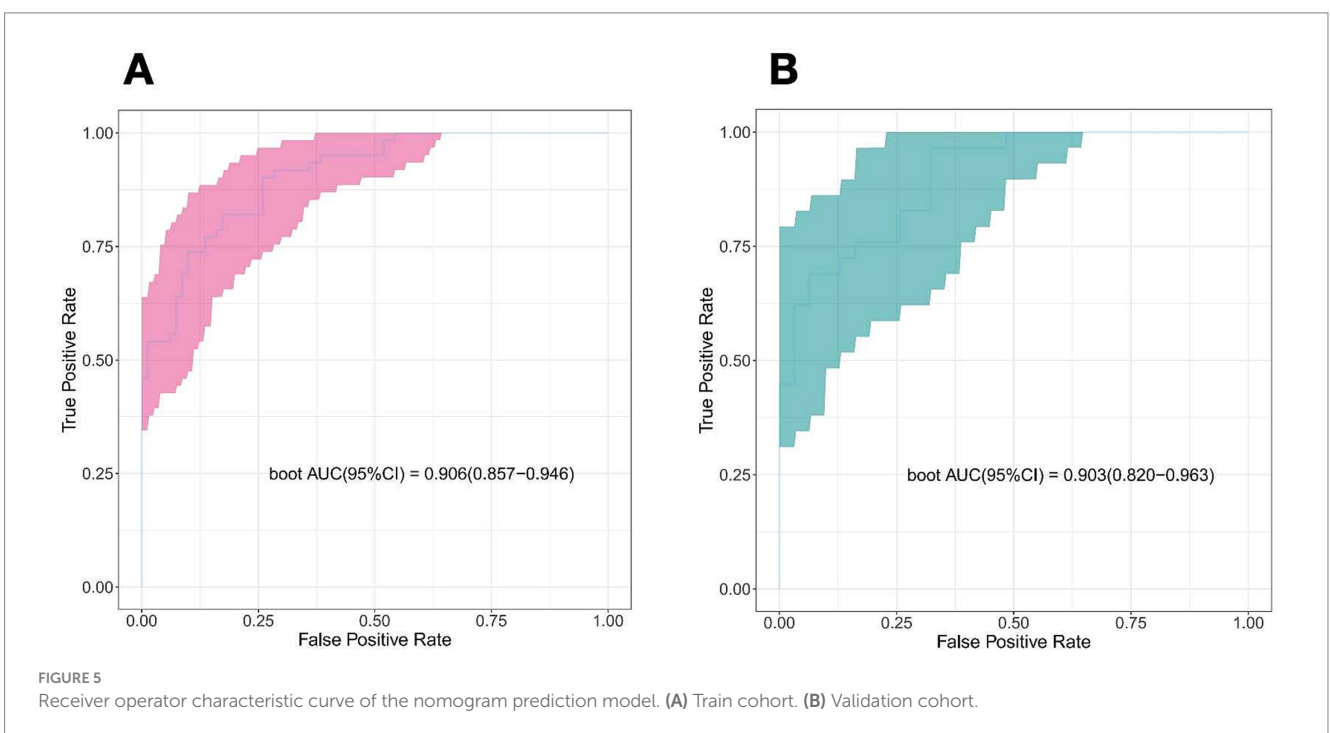
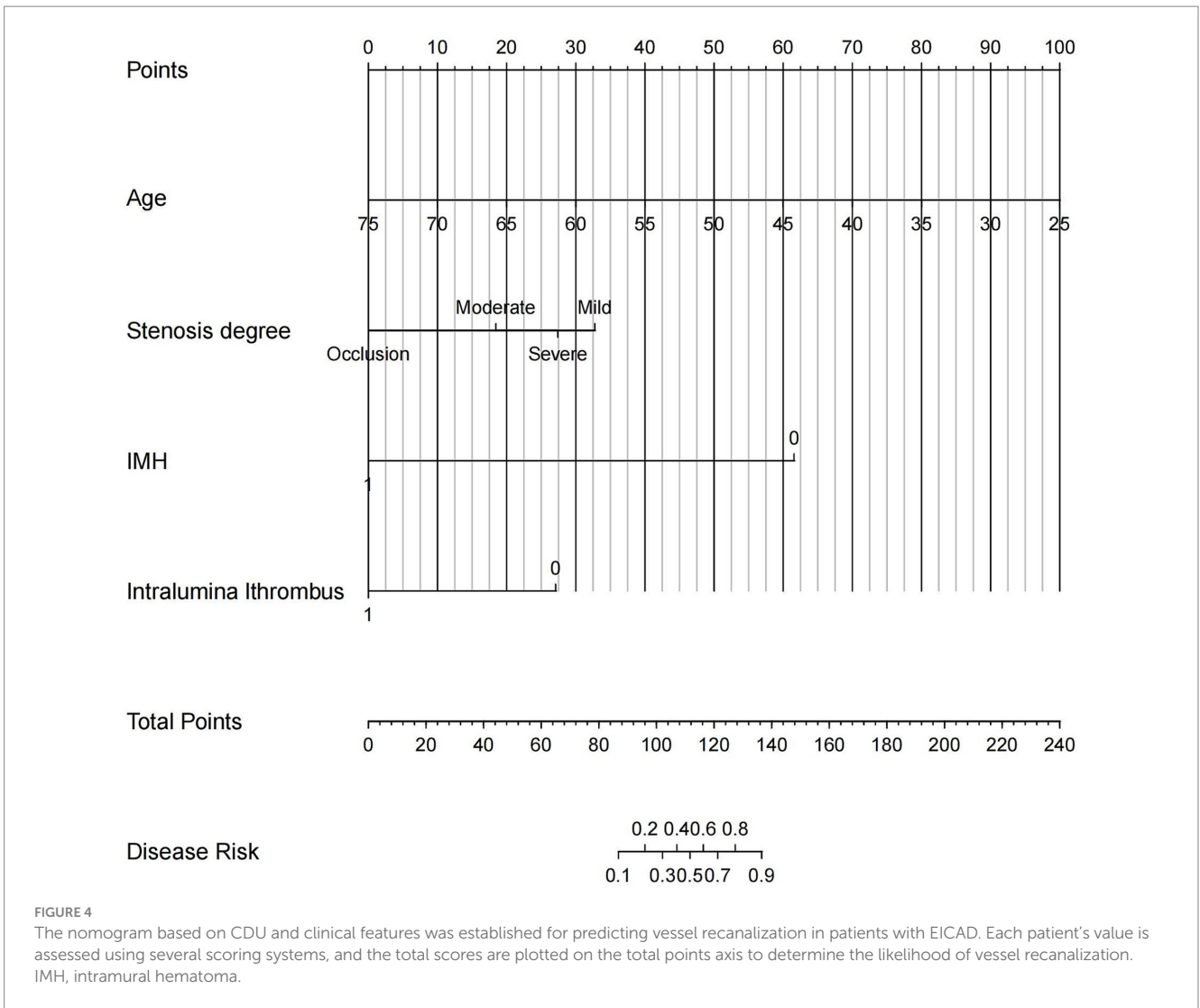
Discussion

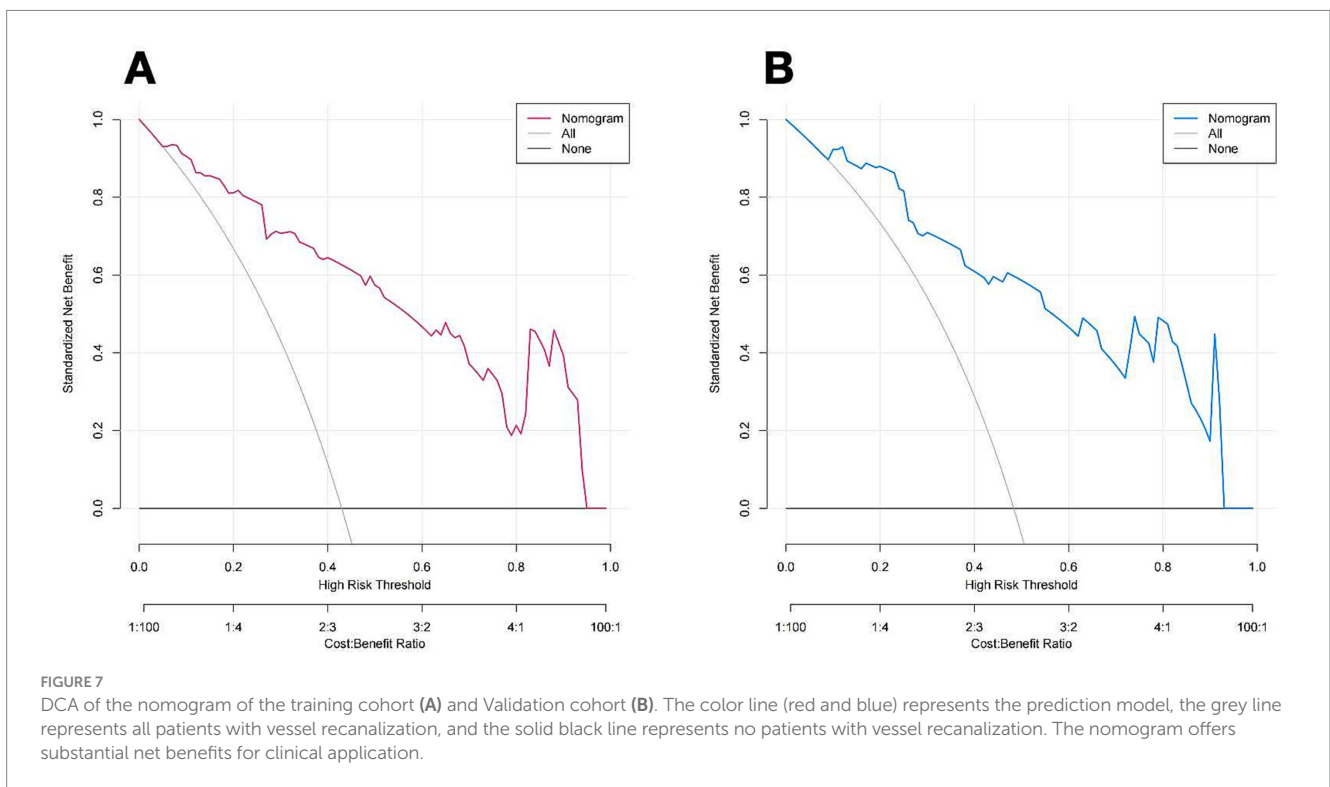
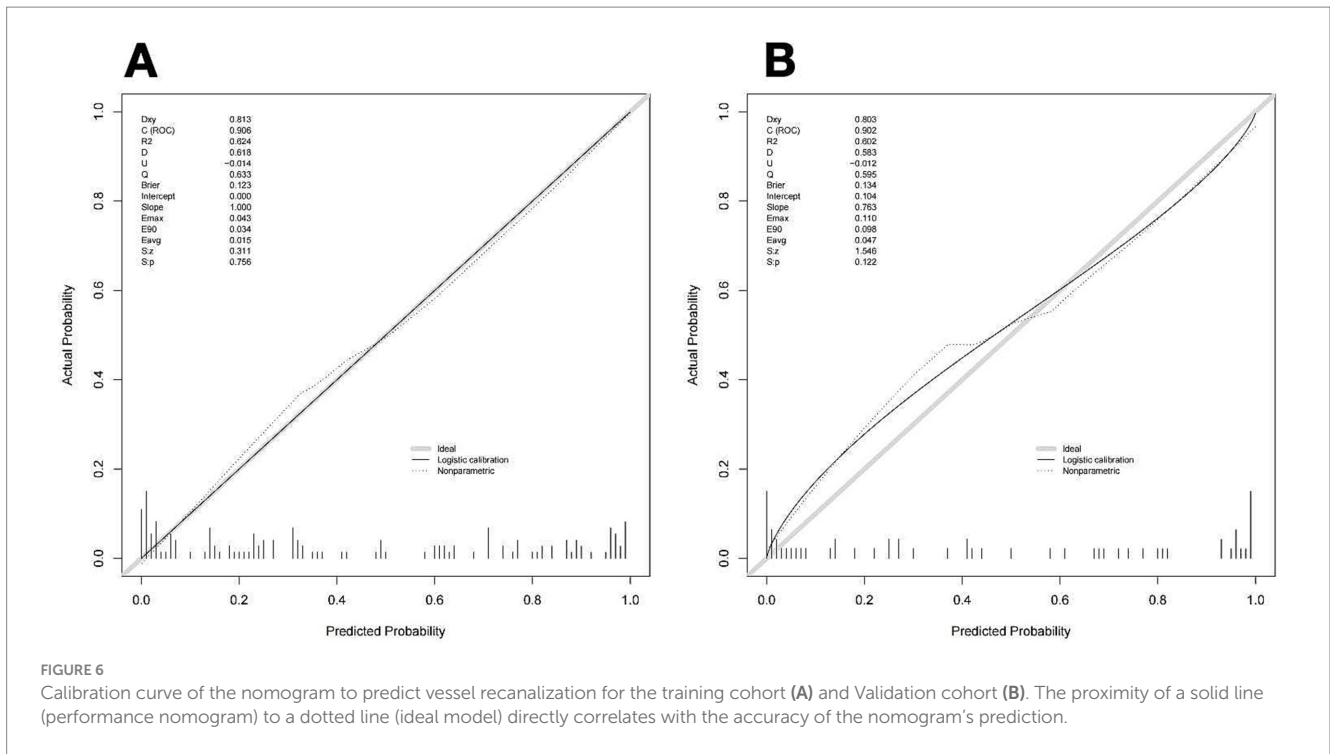
In the current paper, we created a nomogram that utilizes CDU features and clinical parameters for forecasting vessel recanalization in EICAD patients. This nomogram was verified by analyzing ROC, calibration, DCA curves, and CIC for both the training set and validation set. The outcomes manifested in the nomogram may represent a useful tool for predicting vessel recanalization. Baracchini et al. analyzed 103 ICAD and VAD patients and concluded that the recanalization rates were 55.0% (33/60) and 46.5% (20/43), respectively (5). The prognosis of patients with CAD is strongly

influenced by vessel recanalization, and clarifying the influencing factors of recanalization helps predict the recanalization rate and evaluate the prognosis of patients. Our findings underscore the clinical relevance of vessel recanalization in EICAD. The significantly lower incidence of cerebrovascular events in patients with recanalization (3.3% vs. 11.6%) suggests that successful recanalization may mitigate long-term thromboembolic risk. This aligns with prior studies reporting that persistent arterial occlusion in CAD is associated with higher stroke recurrence rates (16).

Some studies have used ultrasound to follow up patients with cervical artery dissection to explore the related factors of recanalization. Strunk et al. analyzed 183 dissected vessels and found that the number of dissecting vessels and the degree of lumen stenosis were independent risk factors (17). However, few studies have been reported to predict EICAD vessel recanalization by combining CDU features and clinical characteristics. Our results found that age, intramural hematoma, Intraluminal thrombus, and lumen stenosis degree were predictors of vessel recanalization. LASSO regression analysis can solve a variety of confounding variables as well as multicollinearity problems, thus providing a more accurate result. In addition, the LASSO can also filter the variables, making the model relatively simple and stable. The primary distinction between our work and other studies using logistic regression analysis is that we used LASSO regression analysis to screen the variables and combined traditional logistic regression analysis to obtain a more comprehensive model, thereby improving the prediction efficacy.

A previous study of 110 patients with vertebral artery dissections reported that younger patients had better clinical outcomes than older patients (18), which is consistent with our results. Our results showed that age was negatively correlated with vessel recanalization. Results from the CADISS trial also showed a significant association between increasing age and residual lumen stenosis and occlusion (19). The reasons may be as follows: the absorption of hematoma in CAD depends on fibrinolysis, while the function of the human fibrinolytic system is related to age, with the strongest effect in youth, and its function gradually decreases with the growth of age (20, 21). Some





studies have reported that with the increase in age, the decrease of male androgen and female estrogen levels can lead to a decrease in fibrinolytic system activity (22, 23). Therefore, in older patients, the function of the fibrinolytic system is relatively reduced, with the dissolution and absorption of the intramural hematoma weakened, which eventually leads to the failure of vessel recanalization.

Some studies have reported that smoking may lead to CAD. Our study showed that smoking is negatively correlated with

vascular recanalization, and the probability of vascular recanalization in smokers is significantly lower than that in non-smokers. The reason maybe that smoking can cause vascular smooth muscle proliferation, and vascular smooth muscle proliferation plays an important role in the occurrence, development and prognosis of vascular diseases (24, 25). Smoking will cause vasculitic changes, resulting in changes in the structure of blood vessels, which will affect the adhesion of the inner artery

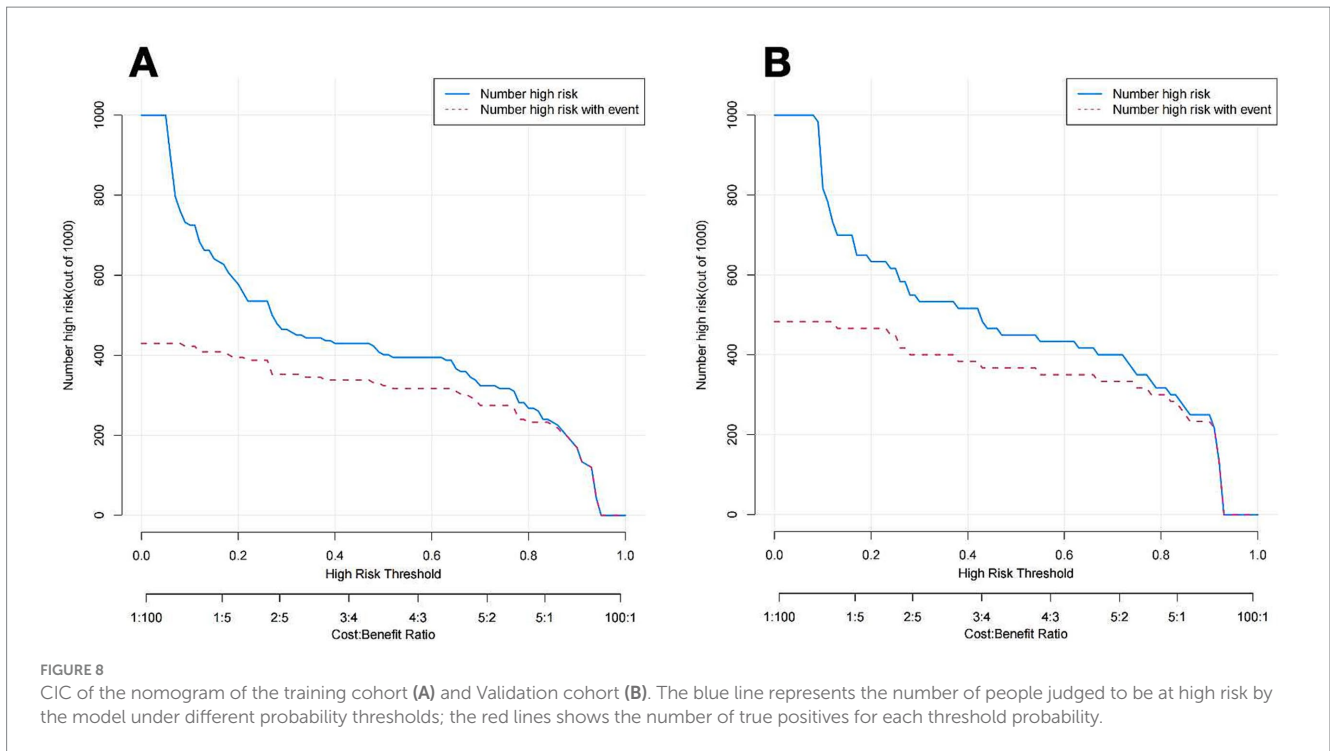


FIGURE 8 CIC of the nomogram of the training cohort (A) and Validation cohort (B). The blue line represents the number of people judged to be at high risk by the model under different probability thresholds; the red lines shows the number of true positives for each threshold probability.

of the dissection blood vessels during the recovery process, and thus hinder the recanalization of the dissection blood vessels (24, 25).

Vicenzini et al. (26) conducted performed a 4-year ultrasound follow-up study on 14 CAD patients and found that degenerative intramural hematoma seemed to be associated with persistent occlusion and partial recanalization. The presence of degenerated hematoma in the carotid artery (CA) indicates that the occlusion can be uneven and recanalized, and the remodeling of intramural hematoma substances can sometimes take up to two years. Our findings showed that IMH may be a risk factor for vessel recanalization. The reason may be that when the hematoma changes to the chronic stage, the echo-intensity is gradually enhanced. The enhanced echo-intensity of the intramural hematoma represents the absorption of hemoglobin, as well as fibrosis. At this time, the vascular wall remodeling and the probability of vascular recanalization will be greatly reduced. CDU surveillance is beneficial to the early detection the echo-intensity of IMH, and patients can be treated in time, which is of great significance to improving the vessel recanalization rate.

Our findings showed that the recanalization rate of occlusion was 33.0%, and MVL analysis indicated that vascular occlusion was an autonomous risk factor for complete recanalization. These outcomes corroborate the prior research conducted on CAD patients; the recanalization rate of stenosis is 46 to 90% and about 33 to 50% in patients with occlusion (27). As the lumen of the internal carotid artery is thick, the blood flow is high, and the blood pressure on the wall is large. When the intima of the artery is torn, the blood flow enters the false lumen under the action of high pressure, resulting in more serious intima tear and larger intramural hematoma formation, which is easy to cause severe stenosis or occlusion of the internal carotid artery lumen. Traenka et al. examined a total of 2,148 patients from many centers and reached a conclusion that dissection artery occlusion predicted a poorer prognosis and a complete recanalization

rate in CAD patients (28). The reason may be related to the effect of arterial occlusion on vascular remodeling in CAD patients. The remodeling mechanism of arterial vessels is related to the shear force of the vascular wall. When CAD only causes arterial stenosis, the decrease in vessel diameter leads to an increase in vascular wall shear force, and the increased shear force can activate nitric oxide-dependent vasodilation, inhibit endothelial cell proliferation and inflammatory response, stabilize vascular endothelial cells, and enlarge the inner diameter of the artery cavity, then promote CAD vascular cavity complete recanalization (29–31).

The nomogram we have created has several clinical implications. Initially, based on the information available to us, this is the first nomogram to serve as a non-invasive tool based on CDU and clinical characteristics to predict vessel recanalization in patients with EICAD, aiding in better risk stratification. Moreover, the nomogram’s high-risk threshold (probability <50%) identifies patients with a low likelihood of spontaneous recanalization, who may benefit from intensified monitoring or early endovascular intervention. Future trials could validate whether targeting high-risk patients with adjunct therapies improves outcomes.

There are many constraints in our research that need to be recognized. Initially, the cohort consisted of patients only from a single facility, and the sample size was rather limited, perhaps limiting its representativeness to the broader community. Furthermore, the nomogram underwent validation in people from the same institution that produced the training cohort; external validation in diverse populations will be essential to confirm the generalizability of our findings. Future research should aim to validate our nomogram externally in different populations and settings. Additionally, integrating novel predictors or biomarkers could enhance the predictive accuracy of the nomogram, warranting further investigation. Lastly, treatment regimens (e.g., duration, phase-based adjustments, and compliance) were not systematically recorded in this retrospective study, which may have influenced recanalization

outcomes. Future studies should prospectively control for therapeutic variables.

Conclusion

We constructed a user-friendly and non-invasive nomogram based on CDU and clinical features to predict vessel recanalization in EICAD patients, which may facilitate early clinical evaluation to select individual therapies and thus improve patient outcomes.

Data availability statement

The raw data supporting the conclusions of this article will be made available by the authors, without undue reservation.

Ethics statement

The studies involving humans were approved by Ethics Committee of the first affiliated hospital of Soochow University. The studies were conducted in accordance with the local legislation and institutional requirements. Written informed consent for participation in this study was provided by the participants' legal guardians/next of kin.

Author contributions

XX: Conceptualization, Data curation, Investigation, Methodology, Software, Writing – original draft, Writing – review &

editing. YY: Conceptualization, Methodology, Writing – review & editing. YQ: Validation, Visualization, Writing – review & editing. LZ: Writing – review & editing. PH: Conceptualization, Funding acquisition, Project administration, Writing – original draft, Writing – review & editing.

Funding

The author(s) declare that financial support was received for the research and/or publication of this article. This study was supported by people's livelihood science and technology project (research on application of key technologies) of Suzhou (No. SS202061), and Technical cooperation project of Soochow University (No. H211064).

Conflict of interest

The authors declare that the research was conducted in the absence of any commercial or financial relationships that could be construed as a potential conflict of interest.

Publisher's note

All claims expressed in this article are solely those of the authors and do not necessarily represent those of their affiliated organizations, or those of the publisher, the editors and the reviewers. Any product that may be evaluated in this article, or claim that may be made by its manufacturer, is not guaranteed or endorsed by the publisher.

References

- Scopelliti G, Karam A, Labreuche J, Bricout N, Marrama F, Diomedei M, et al. Internal carotid artery patency after mechanical thrombectomy for stroke due to occlusive dissection: impact on outcome. *Eur Stroke J.* (2023) 8:199–207. doi: 10.1177/23969873221140649
- Debette S, Leys D. Cervical-artery dissections: predisposing factors, diagnosis, and outcome. *Lancet Neurol.* (2009) 8:668–78. doi: 10.1016/S1474-4422(09)70084-5
- Rodallec MH, Marteau V, Gerber S, Desmottes L, Zins M. Craniocervical arterial dissection: spectrum of imaging findings and differential diagnosis. *Radiographics.* (2008) 28:1711–28. doi: 10.1148/rg.286085512
- Bachmann R, Nassenstein I, Kooijman H, Dittrich R, Kugel H, Niederstadt T, et al. Spontaneous acute dissection of the internal carotid artery: high-resolution magnetic resonance imaging at 3.0 tesla with a dedicated surface coil. *Investig Radiol.* (2006) 41:105–11.
- Nedeltchev K, Bickel S, Arnold M, Sarikaya H, Georgiadis D, Sturzenegger M, et al. R2-recanalization of spontaneous carotid artery dissection. *Stroke.* (2009) 40:499–504. doi: 10.1161/STROKEAHA.108.519694
- Wessels T, Mosso M, Krings T, Klotzsch C, Harrer JU. Extracranial and intracranial vertebral artery dissection: long-term clinical and duplex sonographic follow-up. *J Clin Ultrasound.* (2008) 36:472–9. doi: 10.1002/jcu.20511
- Baracchini C, Tonello S, Meneghetti G, Ballotta E. Neurosonographic monitoring of 105 spontaneous cervical artery dissections: a prospective study. *Neurology.* (2010) 75:1864–70. doi: 10.1212/WNL.0b013e3181feae5e
- Yaghi S, Engelter S, Del Brutto VJ, Field TS, Jadhav AP, Kicieliński K, et al. Treatment and outcomes of cervical artery dissection in adults: a scientific statement from the American Heart Association. *Stroke.* (2024) 55:e91–e106. doi: 10.1161/STR.0000000000000457
- Benninger DH, Baumgartner RW. Ultrasound diagnosis of cervical artery dissection. *Front Neurol Neurosci.* (2006) 21:70–84. doi: 10.1159/000092386
- de Bray JM, Lhoste P, Dubas F, Emile J, Saumet JL. Ultrasonic features of extracranial carotid dissections: 47 cases studied by angiography. *J Ultrasound Med.* (1994) 13:659–64. doi: 10.7863/jum.1994.13.9.659
- Hunter MA, Santosh C, Teasdale E, Forbes KP. High-resolution double inversion recovery black-blood imaging of cervical artery dissection using 3T MR imaging. *AJNR Am J Neuroradiol.* (2012) 33:E133–7. doi: 10.3174/ajnr.A2599
- Coppenrath E, Lenz O, Sommer N, Lummel N, Linn J, Treitl K, et al. Clinical significance of intraluminal contrast enhancement in patients with spontaneous cervical artery dissection: a black-blood MRI study. *Rofo.* (2017) 189:624–31. doi: 10.1055/s-0043-104632
- Hanning U, Sporns PB, Schmiedel M, Ringelstein EB, Heindel W, Wiendl H, et al. CT versus MR techniques in the detection of cervical artery dissection. *J Neuroimaging.* (2017) 27:607–12. doi: 10.1111/jon.12451
- Mehdi E, Aralasmak A, Toprak H, Yildiz S, Kurtcan S, Kolukisa M, et al. Craniocervical dissections: radiologic findings, pitfalls, mimicking diseases: a pictorial review. *Curr Med Imaging Rev.* (2018) 14:207–22. doi: 10.2174/1573405613666170403102235
- Ferguson GG, Eliasziw M, Barr HW, Clagett GP, Barnes RW, Wallace MC, et al. The north American symptomatic carotid endarterectomy trial: surgical results in 1415 patients. *Stroke.* (1999) 30:1751–8. doi: 10.1161/01.STR.30.9.1751
- Lounsbury E, Niznick N, Mallick R, Dewar B, Davis A, Fergusson DA, et al. Recurrence of cervical artery dissection: a systematic review and meta-analysis. *Int J Stroke.* (2024) 19:388–96. doi: 10.1177/17474930231201434
- Strunk D, Schwindt W, Wiendl H, Dittrich R, Minnerup J. Long-term Sonographical follow-up of arterial stenosis due to spontaneous cervical artery dissection. *Front Neurol.* (2021) 12:792321. doi: 10.3389/fneur.2021.792321
- Arnold M, Boussier MG, Fahrni G, Fischer U, Georgiadis D, Gandjour J, et al. Vertebral artery dissection: presenting findings and predictors of outcome. *Stroke.* (2006) 37:2499–503. doi: 10.1161/01.STR.0000240493.88473.39
- Markus HS, Levi C, King A, Madigan J, Norris J. Cervical artery dissection in stroke study I: antiplatelet therapy vs anticoagulation therapy in cervical artery dissection: the cervical artery dissection in stroke study (CADISS) randomized clinical trial final results. *JAMA Neurol.* (2019) 76:657–64. doi: 10.1001/jamaneurol.2019.0072

20. Kwaan HC. From fibrinolysis to the plasminogen-plasmin system and beyond: a remarkable growth of knowledge, with personal observations on the history of fibrinolysis. *Semin Thromb Hemost.* (2014) 40:585–91. doi: 10.1055/s-0034-1383545
21. Ochi A, Adachi T, Inokuchi K, Ogawa K, Nakamura Y, Chiba Y, et al. Effects of aging on the coagulation fibrinolytic system in outpatients of the cardiovascular department. *Circ J.* (2016) 80:2133–40. doi: 10.1253/circj.CJ-16-0530
22. Chistiakov DA, Myasoedova VA, Melnichenko AA, Grechko AV, Orekhov AN. Role of androgens in cardiovascular pathology. *Vasc Health Risk Manag.* (2018) 14:283–90. doi: 10.2147/VHRM.S173259
23. Montt-Guevara MM, Palla G, Spina S, Bernacchi G, Cecchi E, Campelo AE, et al. Regulatory effects of estetrol on the endothelial plasminogen pathway and endothelial cell migration. *Maturitas.* (2017) 99:1–9. doi: 10.1016/j.maturitas.2017.02.005
24. Yaghi S, Maalouf N, Keyrouz SG. Cervical artery dissection: risk factors, treatment, and outcome; a 5-year experience from a tertiary care center. *Int J Neurosci.* (2012) 122:40–4. doi: 10.3109/00207454.2011.622453
25. Debette S, Metso T, Pezzini A, Abboud S, Metso A, Leys D, et al. Association of vascular risk factors with cervical artery dissection and ischemic stroke in young adults. *Circulation.* (2011) 123:1537–44. doi: 10.1161/CIRCULATIONAHA.110.000125
26. Vicenzini E, Toscano M, Maestrini I, Petolicchio B, Lenzi GL, Di Piero V. Predictors and timing of recanalization in intracranial carotid artery and siphon dissection: an ultrasound follow-up study. *Cerebrovasc Dis.* (2013) 35:476–82. doi: 10.1159/000350212
27. Patel RR, Adam R, Maldjian C, Lincoln CM, Yuen A, Arneja A. Cervical carotid artery dissection: current review of diagnosis and treatment. *Cardiol Rev.* (2012) 20:145–52. doi: 10.1097/CRD.0b013e318247cd15
28. Traenka C, Grond-Ginsbach C, Goeggel Simonetti B, Metso TM, Debette S, Pezzini A, et al. Artery occlusion independently predicts unfavorable outcome in cervical artery dissection. *Neurology.* (2020) 94:e170–80. doi: 10.1212/WNL.0000000000008654
29. Lee WJ, Jung KH, Moon J, Lee ST, Chu K, Lee SK, et al. Prognosis of spontaneous cervical artery dissection and transcranial Doppler findings associated with clinical outcomes. *Eur Radiol.* (2016) 26:1284–91. doi: 10.1007/s00330-015-3944-4
30. Garanich JS, Pahakis M, Tarbell JM. Shear stress inhibits smooth muscle cell migration via nitric oxide-mediated downregulation of matrix metalloproteinase-2 activity. *Am J Physiol Heart Circ Physiol.* (2005) 288:H2244–52. doi: 10.1152/ajpheart.00428.2003
31. Cheng C, Tempel D, van Haperen R, van der Baan A, Grosveld F, Daemen MJ, et al. Atherosclerotic lesion size and vulnerability are determined by patterns of fluid shear stress. *Circulation.* (2006) 113:2744–53. doi: 10.1161/CIRCULATIONAHA.106.652222